Article

Fog Droplet Collection by Corona Discharge in a Needle–Cylinder Electrostatic Precipitator with a Water Cooling System

Hui Fu [ID], Wenyi Xu, Zhen Liu and Keping Yan *

College of Chemical and Biological Engineering, Zhejiang University, Hangzhou 310028, China; fh1990@zju.edu.cn (H.F.); 21928141@zju.edu.cn (W.X.); zliu@zju.edu.cn (Z.L.)
* Correspondence: kyan@zju.edu.cn

Abstract: In this study, a needle–cylinder electrostatic precipitator with a water cooling system was designed to enhance the harvest of atmospheric water in wet flue gas. The effects of flow rate, temperature and particles on the collection of fog droplets were investigated. Meanwhile, the energy efficiency of water collection was analyzed at different voltages. The results show that the current decreases with the increase of air relative humidity under the same voltage, and the breakdown voltage increases obviously. Concurrently, by appropriately reducing the wet flue gas flow velocity, the residence time of fog droplets in the electric field can be increased, fully charging the droplets and improving the water collection efficiency. Moreover, experiments revealed that through decreasing the flue gas temperature, both the water collection rate and energy efficiency can be improved. In addition, the presence of particles in wet gas can improve the water collection rate by 5~8% at different discharge voltages. Finally, based on energy efficiency analysis, with the increase of voltage, although the water collection rate increased, the energy efficiency decreased.

Keywords: corona discharge; ionic wind; heat exchange; water collection; energy efficiency

1. Introduction

Currently, the environmental impact of wet plume emissions caused by coal combustion in thermal power units and industrial boilers has attracted widespread attention [1]. In recent years, various provinces and cities in China have released policies on wet plume treatment. The generation of wet plumes is related to the external environment and the state of the exhausted flue gas [2]. The commonly used treatment technologies include flue gas condensation technology, flue gas heating technology and flue gas condensation reheating technology [3]. To date, different methods have been developed and investigated for flue gas dehumidification, including the cold condensing dehumidification method [4,5], membrane dehumidification technology [6] and the absorption method [7]. Among them, mist collectors are the current technology used to recover moisture from flue gas; they make use of a mesh to block the mist flow, allowing fog droplets to stick and fall into the collector [8]. At present, the experimentally measured collection efficiency of the mesh fog collector is approximately 10–30% [9,10]. Water vapor is also collected from the atmosphere by devices called atmospheric water generators (AWGs). Most AWGs can drive air to its dew point by using Peltier cells or heat exchangers to enhance condensation, thus producing liquid water [11]. Although the current "wet smoke plume" treatment technology has made some progress, it is limited by the environment and flue gas conditions. Moreover, the recovery efficiency of waste heat and water is still low, so how to efficiently recover heat and water in wet flue gas has become a new challenge for the development of wet plume treatment technology.

Electrohydrodynamics (EHD) is related to a type of low-temperature plasma in plasma science and ionic wind generators (IWGs) are the application of the EHD phenomenon [12].

The advantages of ionic wind include fast response [13], low-cost maintenance [14] and low-energy consumption [15]. Ionic wind, namely the secondary flow induced by an electric field, is a physical phenomenon caused by the collision between charged particles and gas molecules produced by corona discharge under a nonuniform electric field. Ionic wind generated by corona discharge has been intensively applied for heat transfer enhancement for many years [13,16–21], for it can disturb the boundary layer on the airside of the heat exchanger [22,23]. The principle of electrostatically enhanced fog collection is similar to that of the electrostatic precipitator (ESP): by applying an external electric field to ionize the gas, the fog droplets are charged, and these charged droplets are captured on the collection plate under the combined action of the electric field force and drag force of the airflow [22]. Figure 1 shows the principle of electric mist elimination. Moreover, the harvest of atmospheric water by electrostatic means has already been studied for some years. Decades ago, Uchiyama and Jyumonji [24] developed an electrostatic fog-liquefier and proved that it worked successfully by outdoor experiments. Damak et al. [25], inspired by ESPs, proposed a needle–mesh type electrostatic fog collector and conducted experimental tests, achieving a collection efficiency of more than 60%. The effectiveness of IWGs on enhancing fog water collection has been experimentally demonstrated [26]. The numerical evaluation by Yan et al. [27] showed that charging fog droplets by the corona discharge process and collecting fog in an electric field can result in a higher efficiency of fog collection. Zhang et al. [28] found that the corona discharge could promote the growth of small droplets under both supersaturated and subsaturated conditions, and the possible mechanisms are that the droplet growth enhancement is supported by the synergetic effects of the droplet surface charge, external electric field and ionic wind generated by the corona discharge.
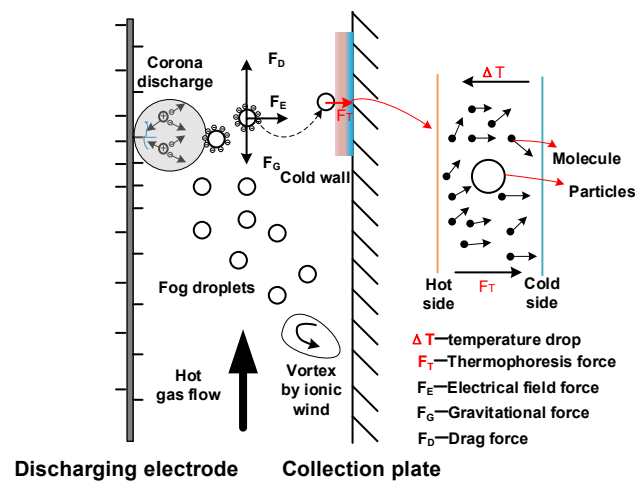

Figure 1. Principle of electric mist elimination.

In short, based on the technology of the ionic wind which enhances heat transfer and fog collection, people can both recover heat from flue gas and lower the temperature, which promotes the growth of small droplets in the fog; then, these grown droplets are collected on the collecting plate under the action of the electric field force by corona discharge. However, there are still few published studies on electrostatically enhanced water collection combining heat exchange and corona discharge. Therefore, a needle–cylinder electrostatic precipitator with a water cooling system was designed in this study, so that we can take advantage of the electric field and temperature drop by a heat exchanger to enhance the harvest of atmospheric water. The effects of flow velocity, temperature and particles on the collection of fog droplets were studied.

2. Experimental System and Methods

2.1. The Experiment Platform

The experimental system in this paper was composed of a high voltage power supply system, heat exchange and corona discharge system, instrument measurement system and pipeline gas distribution system. They are schematically shown in Figures 2 and 3 shows the three-dimensional model of the needle–cylinder electrostatic precipitator with a water cooling system. The size of the needle–cylinder electrostatic precipitator is listed in Table 1. A cross-needle discharge electrode was fixed in the center of the sleeve through the insulator, as shown in Figure 4. The electrode was composed of a supporting tube and a discharge needle. The supporting tube was a stainless-steel tube with a diameter of 8 mm and a total length of 950 mm. A total of 86 electrode needles with a diameter of 1.2 mm and a length of 10 mm were fixed on the supporting tube. The spacing of the needles in the same direction was 42 mm, which was the same as the discharge gap. The tip of the electrode needle is shown in Figure 5. The tip curvature observed by scanning electron microscope was about 150 μm. Compared with the general wire electrode, the curvature of this needle electrode was smaller, and a higher electric field strength could be obtained at the same voltage. A negative high-voltage DC power supply was used in this work. The input voltage was AC 220 V, while the output voltage was 0–60 kV adjustable, and the current could be accurate to 1 μA. The water collecting tank was made of six 5 mm thick organic glass sheets. The size was 250 mm × 250 mm × 120 mm. To explore the strengthening effects of corona discharge on water collection in different hot fluid environments (gas atmosphere, flow rate, temperature, etc.), the gas pipeline system involved in this paper included an air heating system, steam generation system and particle generation system. The three gas pipeline systems were independent of each other. After being fully mixed into the buffer tank, they flowed into the entrance of the needle–cylinder electrostatic precipitator.
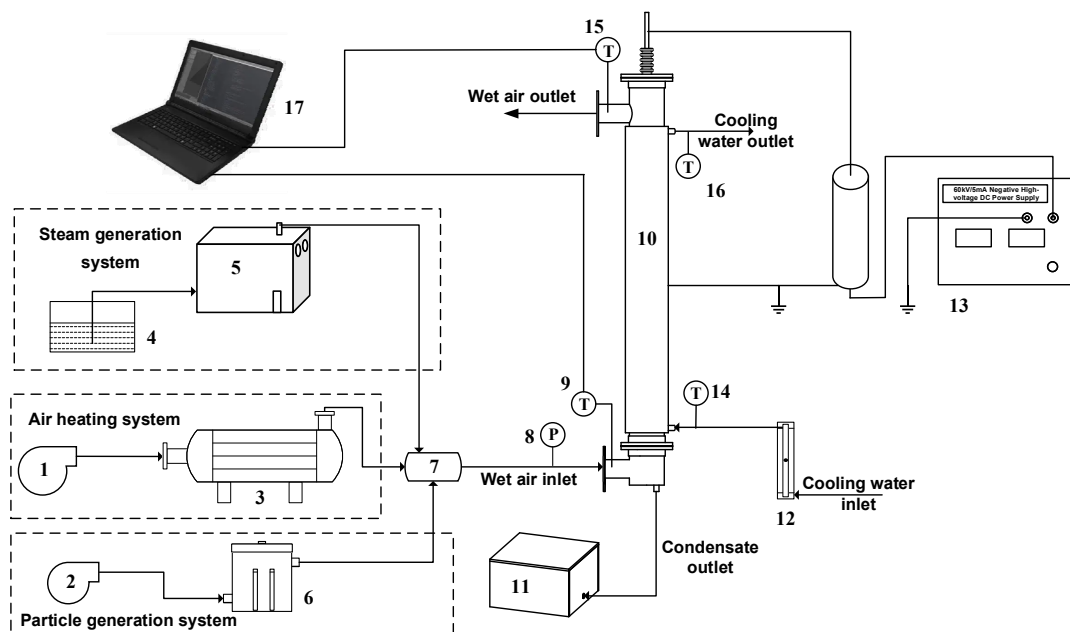

Figure 2. Schematic diagram of experimental setup (1—fan of main pipe line; 2—particle transport fan; 3—air heater; 4—water tank; 5—water vapor generator; 6—particle generator; 7—buffer tank; 8—pressure meter; 9—inlet temperature and humidity sensor; 10—needle–cylinder electrostatic precipitator; 11—water collecting tank; 12—glass rotameter; 13—negative high-voltage DC power supply; 14—inlet thermocouple thermometer; 15—outlet temperature and humidity sensor; 16—outlet thermocouple thermometer; 17—computer).
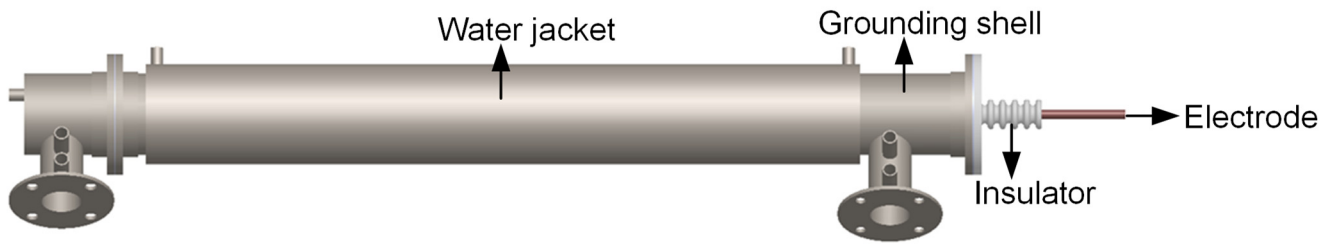
Figure 3. The three-dimensional model of the needle–cylinder electrostatic precipitator with water cooling system.

Table 1. The size of the needle–cylinder electrostatic precipitator.

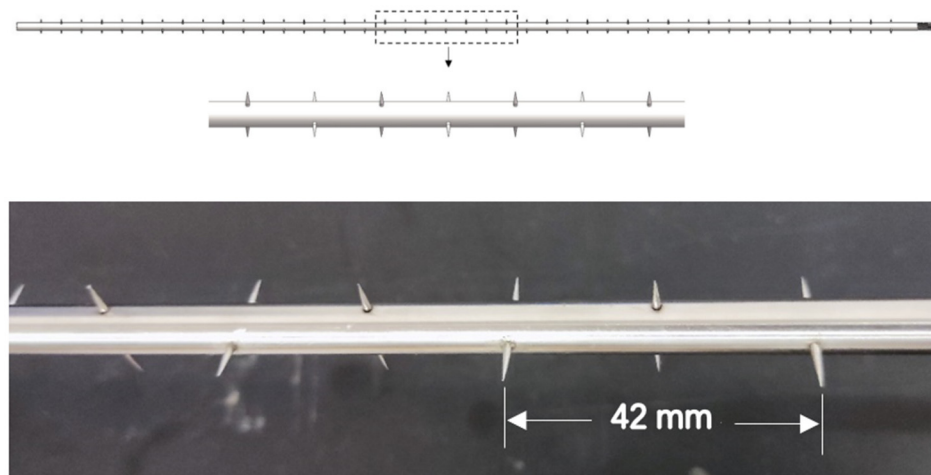|	Inner Diameter (mm)	Outside Diameter (mm)	Wall Thickness (mm)	Length (mm)
Tube side	104	108	2	1100
Shell side	129	133	2	950

Figure 4. Structure diagram of high voltage electrode.

Figure 5. Photo of electrode needle tip.

2.2. Experimental Methods

The relative humidity of the air can be determined by the humidity meter, and the absolute humidity can be calculated by the following formula:

$$H = 622 \frac{\varphi p_s}{P - \varphi p_s} \tag{1}$$

where H is the absolute humidity, g/kg dry air; φ is the relative humidity; P is the total pressure, Pa; and p_s is the saturated vapor pressure of water at this temperature, Pa.

The water collection rate is used to characterize the effect of discharge on water collection.

$$N = \frac{m_{\mathrm{w}}}{\Delta \mathrm{T}} \qquad (2)$$

where N is the amount of water collected per unit time, kg/h; $\Delta \mathrm{T}$ is the discharge time, h; and m_{w} is the water quality collected from the bottom of the heat exchange tube during the discharge time, kg.

Energy efficiency is the amount of water collected per unit energy consumption during the discharge process.

$$\eta = 1000 \frac{N}{P} = 1000 \frac{N}{UI} \qquad (3)$$

where η is the amount of water collected per unit energy consumption, kg/Wh; P is the discharge power, W; U is the voltage, kV; and I is the current, mA.

3. Results and Discussion

3.1. The Discharge Characteristics of the Needle–Cylinder Electrostatic Precipitator in Wet Air

Figure 6 shows the voltammetric characteristic curve of the corona discharge in the heat exchange tube under different air humidity while the inlet temperature of the wet air was kept at 70 °C and air flow rate was 0.72 m/s. The figure shows that the current decreased with the increase of air relative humidity under the same voltage, and the breakdown voltage increased obviously. When the relative humidity was 7%, 50% and 90%, the current at −16 kV was 1683, 1107 and 910 μA, respectively, and the breakdown voltage was about 20, 24 and 26 kV, respectively. This is because water molecules in the air are easy to adsorb and trap free electrons, which reduces the number of free charges and the discharge current. At the same time, it increases the corona voltage of the discharge. It was found in the experiment that the corona voltage of the discharge was about 4.5 kV in the wet air environment, which was 0.7 kV lower than that in the dry air environment. The reason is that the density of wet air is smaller than that of dry air, and the density gradually decreases with the increase of humidity, resulting in the increase of molecular free path and the increase of kinetic energy obtained by electron acceleration. In addition, during the cooling and condensation process of wet air, some droplets adhere to the surface of the corona electrode and distort under the action of the electric field, so that the local electric field is enhanced [29]. Moreover, the droplets on the surface of metal electrodes can reduce the surface barrier, which weakens the hindrance of the surface barrier to free electrons [30]. The above factors lead to the decrease of corona onset voltage in wet air.
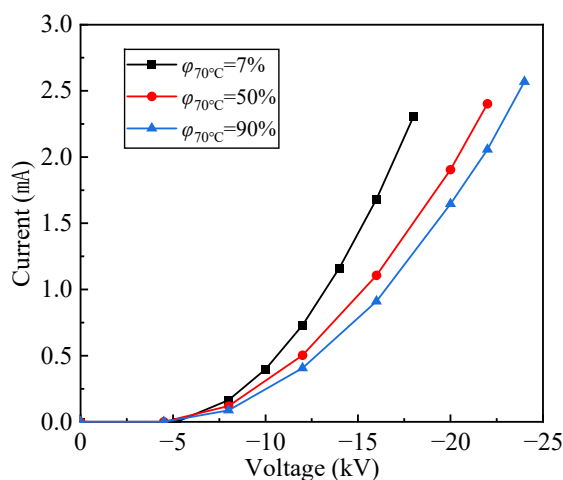

Figure 6. The voltammetric characteristic curves of corona discharge in wet air.

3.2. The Effect of Gas Flow Velocity on Fog Water Collection

The effect of gas flow velocity on fog water collection was measured with the heat exchange and corona discharge system being open. The fog water collection rate at various gas flow velocities under the inlet temperature of the wet air at 70 °C, cooling water at 20 °C and the relative humidity of 67% is shown in Figure 7.

Figure 7 shows that when there was no external electric field, a certain amount of condensed water in the heat exchange tube was collected, and the sources of this part of the water mainly included the following aspects. When the temperature of the wet air dropped to the dew point and below, the water vapor condensed, collided with the droplets in the wet air and gathered and formed large droplets, which sank to the bottom of the heat exchange tube under the action of gravity. The condensed droplets in the falling process captured the droplets in the gas phase and the water vapor condensed on the cold wall surface and flowed out from the bottom of the heat exchange tube. With the increase of the primary flow velocity, the amount of water collected per unit time without an external electric field decreased gradually. This is mainly because the drag force on the droplet increases with the increase of the relative velocity between the droplet and the airflow. As a result, the droplets with a smaller particle size are driven by the airflow and flow out of the heat exchange tube, leading to the decrease of water yield. In addition, with the increase of the flow velocity, the decrease of the relative humidity and the increase of the outlet temperature, the condensation amount of water vapor decreases, which also reduces the total collected water in the heat exchange tube.

As the discharge voltage increased, the water collection rate increased gradually, and the lower the flow rate was, the more obvious the effect of the electric field on the collected water was. Taking −12 kV as an example, when the flow rate was 0.72 m/s, 1.08 m/s, 1.38 m/s and 1.54 m/s, respectively, the water collection rate was increased by 60%, 40%, 22% and 25%, respectively, compared with those without an external electric field. In the strong electric field environment, the liquid particles in wet air are charged in a very short time (a typical charging time constant is 0.01–0.1 s [31]), and gradually move to the wall under the action of the electric field. After reaching the wall, these liquid particles become neutralized and flow downward along the wall under gravity, and finally discharge from the bottom of the heat exchange tube. A higher voltage results in a greater coulomb force on charged droplets, less time being required to move to the wall and more droplets being captured by the electric field at the same residence time, resulting in the greater collection rate of the fog water. In addition, with the increase of voltage, charged droplets with smaller particle sizes condense and form large droplets under the action of the electric field. Meanwhile, the charges of the droplets also increase, making it easier for these droplets to be captured by the electric field to improve the water collection rate. With the increase of flow velocity, the residence time of droplets in the heat exchange tube decreases gradually, and some droplets flow out from the heat exchange tube before reaching the tube wall, which reduces the water collection rate.

Figure 7 indicates that when the flow rate was low, the water collection rate by corona discharge changed little with the increase of voltage. When the flow rate was 0.72 m/s and the voltage increased from −12 kV to −20 kV, the water collection rate increased from 3.16 kg/h to 3.37 kg/h, an increase of 7%. This is because at low flow velocity, the residence time of droplets in the electric field is long enough to allow most of the droplets to be trapped on the tube wall with a lower electric field strength, and the increase in the water collection rate is very limited when the voltage continues to rise. When the flow rate was 0.72–1.38 m/s and the voltage was large enough, the water collection rate of the corona discharge decreased instead, and the phenomenon did not occur when the flow rate was too large. Taking the flow rate of 1.08 m/s as an example, as the voltage raised to −22 kV, the water collection rate was 2.81 kg/h, which was reduced by 7.6% compared with that at −20 kV. When the flow rate was 1.54 m/s, the water collection rate at −22 kV was increased by 5% compared with that at −20 kV. The reason may be that under the condition of a small flow rate, when the voltage is too high, the ionic wind generated by the corona discharge

is intense, and the impact on the movement of liquid particles cannot be ignored. Under the disturbance of ionic wind, some droplets cannot be collected on the wall under the action of the electric field and some droplets are evaporated by the ionic wind [32], so the water collection rate is reduced. When the flow rate is too high, the flow pattern in the tube becomes turbulent, and the disturbance of the ionic wind generated by the corona discharge on the flow field in the tube is small.
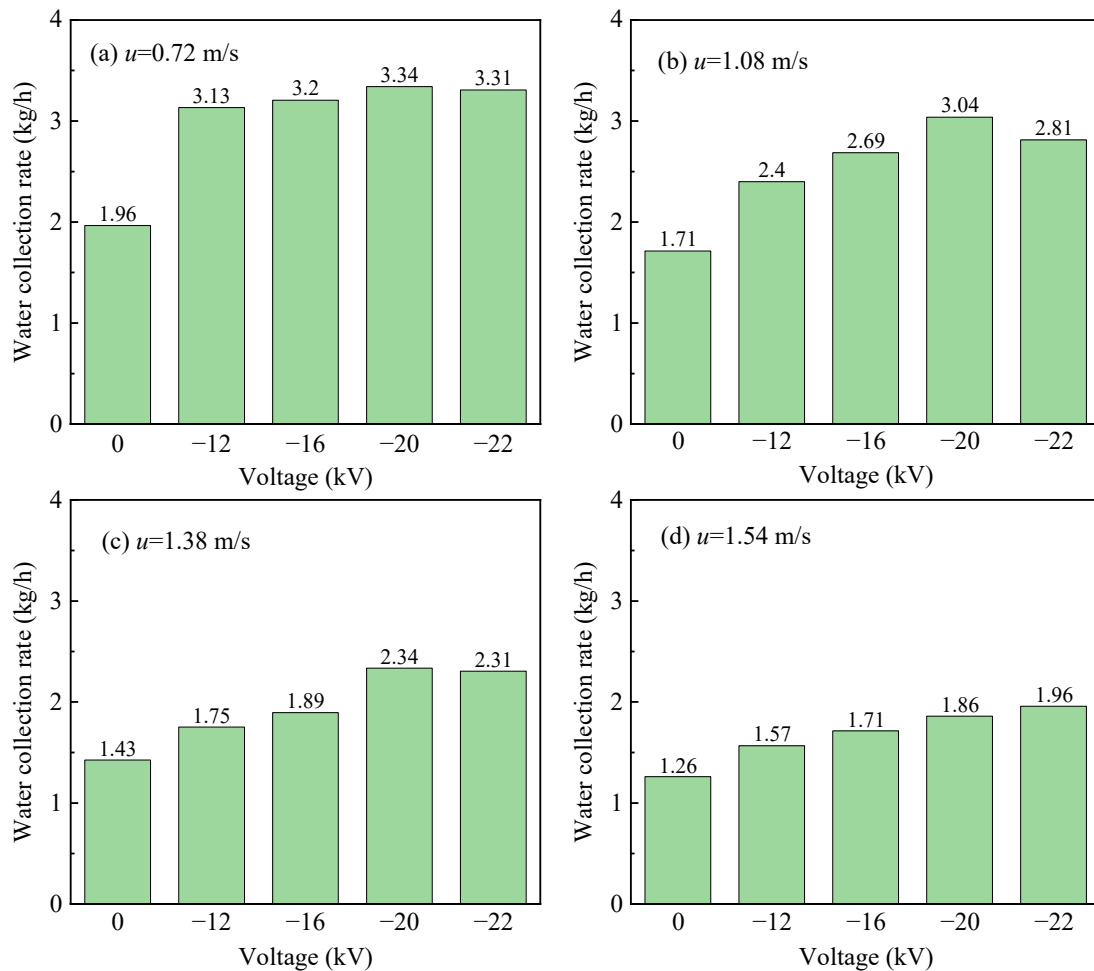

Figure 7. Water collection rate at different flow rates and different voltages. (**a**) the water collection rate at different voltages when the flow velocity was 0.72 m/s. (**b**) the water collection rate at different voltages when the flow velocity was 1.08 m/s. (**c**) the water collection rate at different voltages when the flow velocity was 1.38 m/s. (**d**) the water collection rate at different voltages when the flow velocity was 1.54 m/s.

3.3. The Effect of Temperature on Fog Water Collection

The flue gas temperature will affect discharge characteristics in wet air. Therefore, the effects of corona discharge at different initial temperatures on water collection were investigated. The flow rate was 0.72 m/s, the relative humidity was 67%, the cooling water temperature was about 20 °C and the inlet temperatures were 70 °C and 80 °C.

Figure 8 shows the effect of discharge temperature on the outlet temperature. When the inlet temperatures were 70 °C and 80 °C, as the voltage increased from 0 kV to −22 kV, the outlet temperature drop was 5.88 °C and 3.97 °C, respectively. Figures 9 and 10 show the effect of inlet temperature on the water collection rate and energy efficiency, respectively. It can be seen from the figures that both the water collection rate and energy efficiency decreased with the increase of inlet temperature. With the increase of voltage, the difference between them decreased gradually. When the voltage was 0, −8 and −16 kV, the water

collection rate decreased by 16%, 12% and 5%, respectively. When the voltage was −20 kV, the water collection rate at the two temperatures was almost the same. However, when the voltage was −22 kV, the water collection at the inlet temperature of 80 °C was even higher than that of 70 °C. The experimental results of water collection were basically consistent with the measured temperature and humidity changes. When the voltage is low, the cooling effect caused by the ionic wind is also small, so the outlet temperature and humidity under the inlet temperatures of 80 °C are larger than those at 70 °C, which reduces the water collection rate at higher inlet temperatures. As the voltage increases, the inlet temperature also increases, and the cooling effect of the corona discharge is more obvious, resulting in the outlet temperature and humidity at the two inlet temperatures gradually becoming closer, so that the difference in the effects on the water collection at different temperatures is also reduced. Moreover, when the voltage is high enough, the larger temperature drop leads to a higher water collection rate.
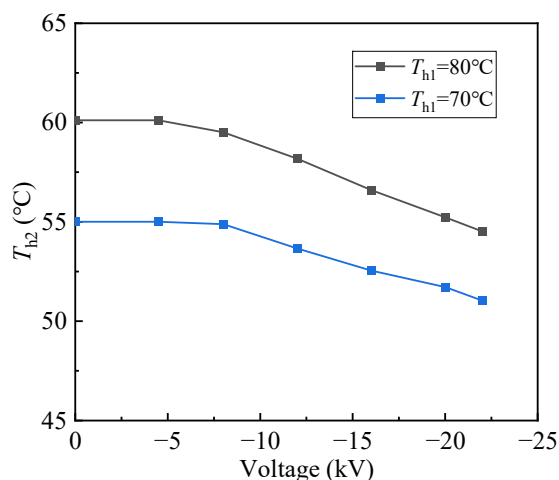
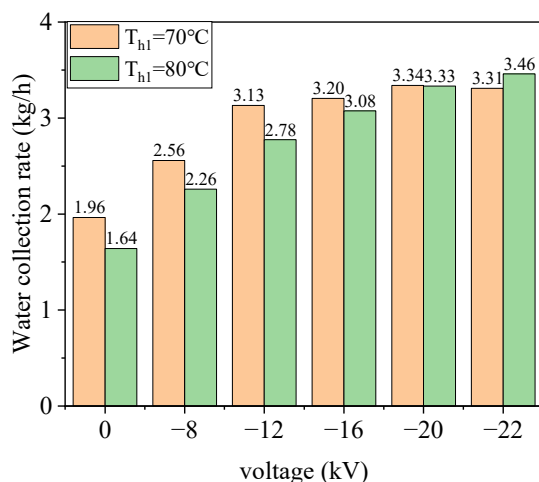**Figure 8.** Effect of discharge temperature on outlet temperature.

Figure 9. Water collection rate at different inlet temperatures.

The above experimental results show that when the air humidity is constant (not saturated), the water collection rate increases to a certain extent with the decrease of the initial temperature. However, under the actual process conditions, the wet flue gas is not necessarily saturated, and when the temperature is high, the water collection effect becomes poor. Although increasing the voltage can effectively improve the water collection rate, the higher the voltage was, the lower the energy efficiency was, as shown in Figure 10. Therefore, it is necessary to reduce the temperature of the flue gas to improve its relative

humidity and improve the recovery efficiency of water resources from the wet flue gas under reasonable conditions.
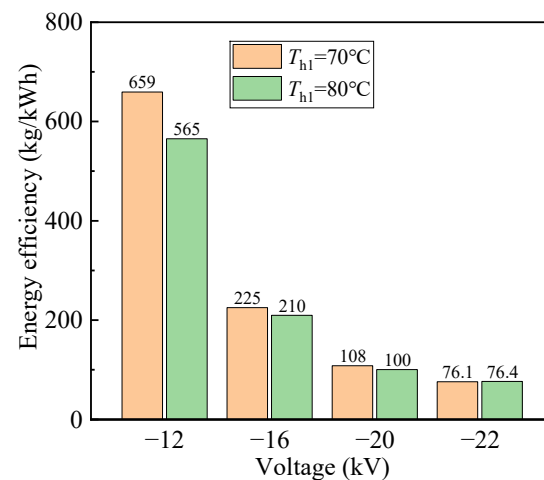

Figure 10. Energy efficiency of water collection at different inlet temperatures.

3.4. The Effect of Fine Particles on Fog Water Collection

In the actual coal-fired power plant, the wet flue gas to be treated may contain a small amount of fine particles remaining after desulfurization and denitrification treatment. The moxibustion smoke particles are fine and submicron particles with diameters from 30 nm to 10 μm [33]; therefore, the moxibustion combustion smoke was taken as the fine particle sample to explore the influence of the existence of particles on the water collection in the wet air environment. In the experiment, the flow velocity of wet air was 1.22 m/s, the inlet temperature was 70 °C, the relative humidity was 67%, the inlet temperature of cooling water was about 20 °C and the flow rate of the cooling water was 100 L/h.

Figure 11 shows the effect of fine particles on the water collection rate. The presence of particles can improve the water collection rate at different discharge voltages. The water collection rate was increased by about 5% after adding particles in the absence of an external electric field. When the operating voltage was −12~−20 kV, the water collection rate was increased by 5~8%, while the water collection rate was increased by about 3% at −22 kV. The effect of particles on water collection can be analyzed from the movement of droplets. Fine particles can be used as the condensation core of supersaturated water vapor in the gas phase, making it condense on the surface of fine particles, promoting the agglomeration of small droplets and forming large droplets that are easy to settle, so that the water collection rate is improved. After the electric field is applied, the charged droplets and particles condense under the action of the electric field, and the mutual agglomeration also improves the water collection effect to a certain extent.

After adding fine particles, corona discharge will capture fine particulate matters while collecting water. Figure 12 shows the color changes of the collected water at different discharge voltages. With the increase of the operating voltage, the color of the collected water gradually changed from light yellow to dark yellow. It can be considered that the content of particulate matters in the water gradually increases with the increase of the voltage. When the electric field is not applied, some of the fine particles act as the condensation core of water vapor, accompanied by collision and coalescence between particles and droplets, and part of the particles are captured during the drop of large droplets [34]. After applying the electric field, the fine particles not captured by the large droplets move to the heat transfer wall under the action of the electric field and are captured by the water film on the wall, resulting in the increase of the particle content in the collected water [35].
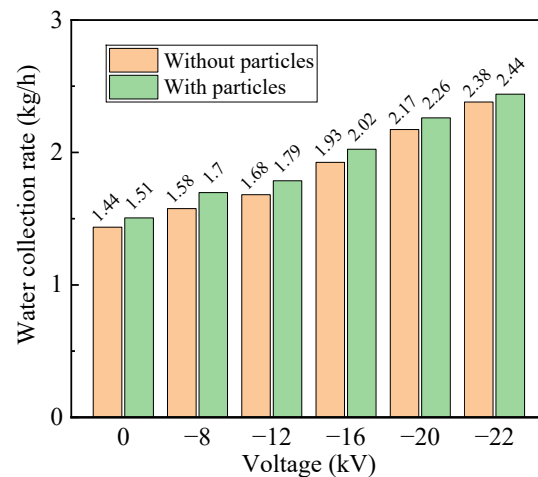
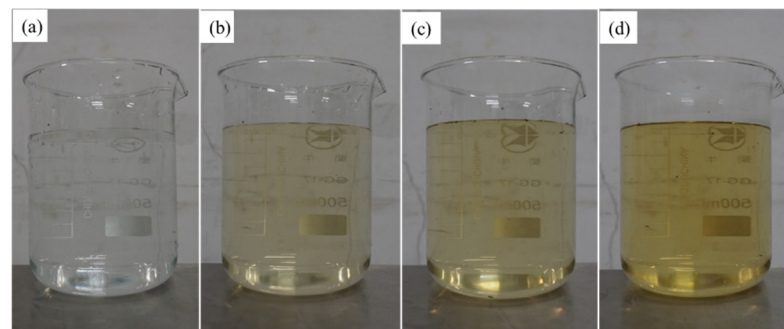**Figure 11.** Effect of fine particles on water collection rate.

Figure 12. Photos of the color changes of collected water at different discharge voltages. (**a**) Without particles. (**b**) with particles at 0 kV. (**c**) with particles at –12 kV. (**d**) with particles at –16 kV.

3.5. Energy Efficiency Analysis

In practical applications, in addition to considering the water collection efficiency, it is also necessary to pay attention to the energy consumption of the system during operation. Taking the results of Section 3.2 as an example, the energy efficiency at different voltages was analyzed, and the results are shown in Figure 13. With the increase of voltage, although the water collection rate increased, the energy efficiency decreased and the amount of water collection per unit energy consumption gradually decreased. Taking the flow rate of 0.72 m/s as an example, when the voltage was −12 kV, −16 kV and −20 kV, the energy water collection per kWh consumed by corona discharge was 645 kg, 219 kg and 102 kg, respectively. This is because part of the energy generated by the corona discharge acts on the fluid to produce ionic wind to strengthen heat transfer, and the other part of the energy is used to drive the droplets to move toward the wall.

The comparison of the economic input and output of the water collection technology by corona discharge at the wet air flow rate of 0.72 m/s is shown in Table 2. This paper only considered the cost of power consumption and cooling water, and the collected water was used to calculate the economic benefits according to the price of industrial water. It can be seen from the table that with the increase of the operation voltage, the economic benefit gradually decreased. When the operation voltage was −12 kV, the income of the collected water obtained by consuming per kWh was 2.64 CNY, and the net income was 2.14 CNY. While the voltage was −20 kV, the net income was negative. It was not feasible to choose this operating condition from an economic point of view.
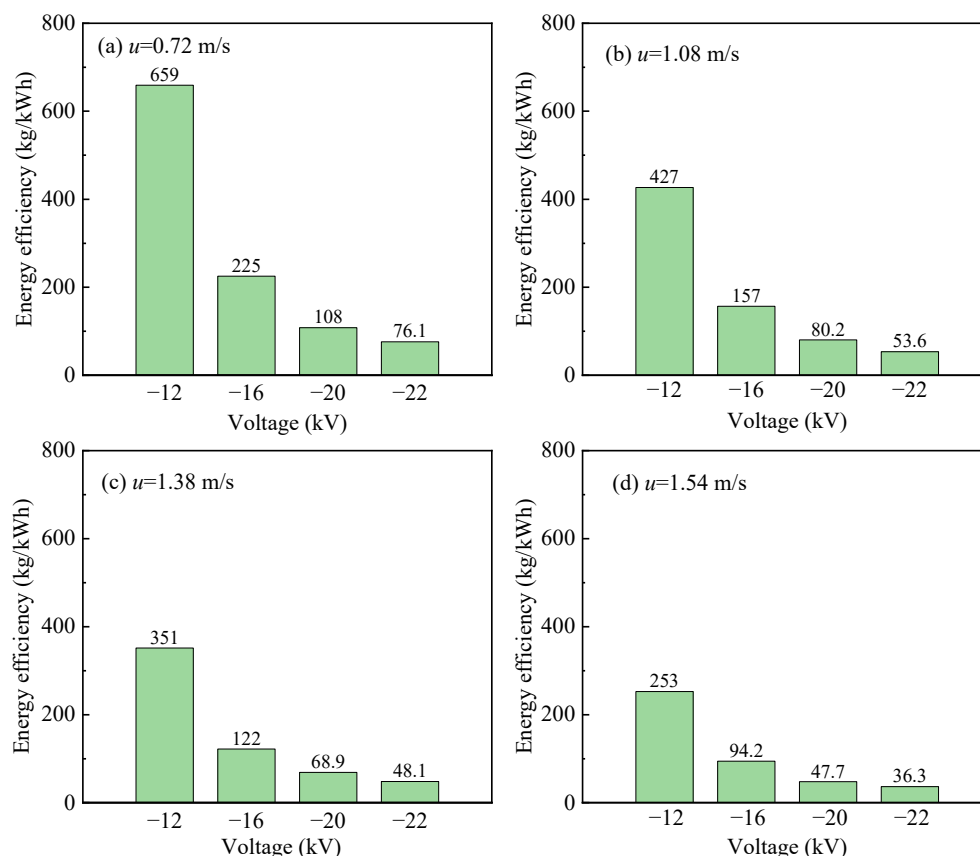
Figure 13. Energy efficiency of water collection at different voltages. (**a**) the energy efficiency at different voltages when the flow velocity was 0.72 m/s. (**b**) the energy efficiency at different voltages when the flow velocity was 1.08 m/s. (**c**) the energy efficiency at different voltages when the flow velocity was 1.38 m/s. (**d**) the energy efficiency at different voltages when the flow velocity was 1.54 m/s.

Table 2. Economic input and output.

Voltage (kV)	−12	−16	−20
Energy efficiency (kg/kWh)	659	225	108
Unit price of industrial water (CNY/t)		4.10	
Income of collected water (CNY/kWh)	2.70	0.92	0.44
Electrovalence (CNY/kWh)		0.50	
Net gain (CNY/kWh)	2.20	0.42	−0.06

4. Conclusions

This paper studied the effects of flow rate, temperature and particles on the collection of fog droplets in a needle–cylinder electrostatic precipitator with a water cooling system. Meanwhile, the energy efficiency of water collection was investigated at different voltages. The main conclusions are listed below:

(1) The current decreased with the increase of air relative humidity under the same voltage, and the breakdown voltage increased obviously; therefore, the relative humidity should be taken into consideration in practice. With the increase of discharge voltage, the water collection rate increased gradually, and the lower the flow velocity was, the more obvious the effect on the water collection by the electric field became. When the voltage was −20 kV and the flow rate was 0.72 m/s, the maximum water collection rate reached 3.34 kg/h, which was 1.7 times that without the electric field. When the inlet temperature decreased, the energy efficiency was improved. As the voltage in-

creases, the inlet temperature also increases, and the cooling effect caused by the ionic wind is more obvious, but the energy efficiency decreases rapidly. When the flow rate was 0.72 m/s and the discharge voltage was -12 kV, the inlet temperature decreased from 80 °C to 70 °C, the water collection rate increased from 2.78 kg/h to 3.13 kg/h and the energy efficiency increased from 565 kg/kWh to 659 kg/kWh; under different voltages, the existence of particles can improve the water collection rate. When the voltage changed from -12 to -20 kV, the water collection rate increased by 5–8%, but when the voltage was -22 kV, the water collection rate increased by about 3%.

(2) Based on energy efficiency analysis, with the increase of voltage, although the water collection rate increased, the energy efficiency decreased. Therefore, the water collection technology by corona discharge needs to comprehensively consider the input (energy consumption), output (water collection benefit) and environmental protection in practical application. When considering economic benefits, the benefits gradually decreased with the increase of voltage. However, from the perspective of environmental protection, the higher the voltage is, the better the water collection effect by corona discharge on wet flue gas becomes, which will reduce the impact of wet plume emissions on the environment.

(3) The above shows that there is an optimization framework needed to determine the optimum condition for the technology to operate and that is the work we will do next. Moreover, due to various factors such as personal time, conditions and technology, there are still some shortcomings which need further research and discussion. The work in this paper was carried out under laboratory conditions, and subsequent scale-up experiments can be carried out to explore the effects on the water collection by corona discharge in a high-flow and high-humidity environment.

Author Contributions: Conceptualization, H.F. and W.X.; methodology, W.X.; investigation, W.X.; resources, K.Y. and Z.L.; data curation, W.X. and H.F.; writing—original draft preparation, H.F.; writing—review and editing, H.F., K.Y. and Z.L. All authors have read and agreed to the published version of the manuscript.

Institutional Review Board Statement: Not applicable.

Informed Consent Statement: Not applicable.

Data Availability Statement: The data presented in this study are available upon request from the corresponding author.

Conflicts of Interest: The authors declare no conflict of interest.

References

1. Shuangchen, M.; Jin, C.; Kunling, J.; Lan, M.; Sijie, Z.; Kai, W. Environmental influence and countermeasures for high humidity flue gas discharging from power plants. *Renew. Sustain. Energy Rev.* **2017**, *73*, 225–235. [CrossRef]
2. Zhang, Y.; Wang, J. Numerical simulation study on the influence of power plant flue gas factors on the formation of white wet plume of flue gas. *IOP Conf. Ser. Earth Environ. Sci.* **2020**, *615*, 012076. [CrossRef]
3. Tyagi, S.K.; Pandey, A.K.; Pant, P.C.; Tyagi, V.V. Formation, potential and abatement of plume from wet cooling towers: A review. *Renew. Sustain. Energy Rev.* **2012**, *16*, 3409–3429. [CrossRef]
4. Feng, Y.; Li, Y.; Cui, L.; Yan, L.; Zhao, C.; Dong, Y. Cold condensing scrubbing method for fine particle reduction from saturated flue gas. *Energy* **2019**, *171*, 1193–1205. [CrossRef]
5. Wang, E.; Li, K.; Husnain, N.; Li, D.; Mao, J.; Wu, W.; Yang, T. Experimental study on flue gas condensate capture and heat transfer in staggered tube bundle heat exchangers. *Appl. Therm. Eng.* **2018**, *141*, 819–827. [CrossRef]
6. Qu, M.; Abdelaziz, O.; Gao, Z.; Yin, H. Isothermal membrane-based air dehumidification: A comprehensive review. *Sustain. Energy Rev.* **2018**, *82*, 4060–4069. [CrossRef]
7. Bai, H.; Zhu, J.; Chu, J.; Chen, X.; Cui, Y.; Yan, Y. Influences of the mixed LiCl-CaCl$_2$ liquid desiccant solution on a membrane-based dehumidification system: Parametric analysis and mixing ratio selection. *Energy Build.* **2019**, *183*, 592–606. [CrossRef]
8. Klemm, O.; Schemenauer, R.S.; Lummerich, A.; Cereceda, P.; Marzol, V.; Corell, D.; Van Heerden, J.; Reinhard, D.; Gherezghiher, T.; Olivier, J.; et al. Fog as a Fresh-Water Resource: Overview and Perspectives. *Ambio* **2012**, *41*, 221–234. [CrossRef]

9. Montecinos, S.; Carvajal, D.; Cereceda, P.; Concha, M. Collection efficiency of fog events. *Atmos. Res.* **2018**, *209*, 163–169. [CrossRef]

10. Park, K.C.; Chhatre, S.S.; Srinivasan, S.; Cohen, R.E.; McKinley, G.H. Optimal design of permeable fiber network structures for fog harvesting. *Langmuir* **2013**, *29*, 13269–13277. [CrossRef]

11. Pontious, K.; Weidner, B.; Guerin, N.; Dates, A.; Pierrakos, O.; Altaii, K. Design of an atmospheric water generator: Harvesting water out of thin air. In Proceedings of the 2016 IEEE Systems and Information Engineering Design Symposium (SIEDS), Charlottesville, VA, USA, 29 April 2016. [CrossRef]

12. Johnson, M.J.; Go, D.B. Recent advances in electrohydrodynamic pumps operated by ionic winds: A review. *Plasma Sources Sci. Technol.* **2017**, *26*, 103002. [CrossRef]

13. Qu, J.; Zhang, D.; Zhang, J.; Tao, W. LED chip cooling system using ionic wind induced by multi-wire corona discharge. *Appl. Therm. Eng.* **2021**, *193*, 116946. [CrossRef]

14. Zhang, Y.; Liu, L.; Chen, Y.; Ouyang, J. Characteristics of ionic wind in needle-to-ring corona discharge. *J. Electrost.* **2015**, *74*, 15–20. [CrossRef]

15. Iranshahi, K.; Martynenko, A.; Defraeye, T. Cutting-down the energy consumption of electrohydrodynamic drying by optimizing mesh collector electrode. *Energy* **2020**, *208*, 118168. [CrossRef]

16. Nelson, D.A.; Zia, S.; Whipple, R.L.; Ohadi, M.M. Corona Discharge Effects on Heat Transfer and Pressure Drop in Tube Flows. *J. Enhanc. Heat Transf.* **2000**, *7*, 81–95. [CrossRef]

17. Wangnipparnto, S.; Tiansuwan, J.; Kiatsiriroat, T.; Wang, C.C. Performance analysis of thermosyphon heat exchanger under electric field. *Energy Convers. Manag.* **2003**, *44*, 1163–1175. [CrossRef]

18. Owsenek, B.L.; Seyed-Yagoobi, J.; Page, R.H. Experimental Investigation of Corona Wind Heat Transfer Enhancement with a Heated Horizontal Flat Plate. *J. Heat Transf.* **1995**, *117*, 309–315. [CrossRef]

19. Ohadi, M.M.; Nelson, D.A.; Zia, S. Heat transfer enhancement of laminar and turbulent pipe flow via corona discharge. *Int. J. Heat Mass Transf.* **1991**, *34*, 1175–1187. [CrossRef]

20. Shin, D.H.; Kim, S.; Ko, H.S.; Shin, Y. Performance enhancement of heat recovery from engine exhaust gas using corona wind. *Energy Convers. Manag.* **2018**, *173*, 210–218. [CrossRef]

21. Wang, J.; Fu, R.; Hu, X. Experimental study on EHD heat transfer enhancement with a wire electrode between two divergent fins. *Appl. Therm. Eng.* **2019**, *148*, 457–465. [CrossRef]

22. Qu, J.; Zeng, M.; Zhang, D.; Yang, D.; Wu, X.; Ren, Q.; Zhang, J.F. A review on recent advances and challenges of ionic wind produced by corona discharges with practical applications. *J. Phys. D: Appl. Phys.* **2021**, *55*, 153002. [CrossRef]

23. Shin, D.H.; Jang, D.K.; Sohn, D.K.; Ko, H.S. Control of boundary layer by ionic wind for heat transfer. *Int. J. Heat Mass Transf.* **2019**, *131*, 189–195. [CrossRef]

24. Uchiyama, H.; Jyumonji, M. Development of an Electrostatic Fogliquefier and Its Field Experiments. *Jpn. J. Appl. Phys.* **1989**, *28*, 2319–2320. [CrossRef]

25. Damak, M.; Varanasi Kripa, K. Electrostatically driven fog collection using space charge injection. *Sci. Adv.* **2018**, *4*, eaao5323. [CrossRef]

26. Cruzat, D.; Jerez-Hanckes, C. Electrostatic fog water collection. *J. Electrost.* **2018**, *96*, 128–133. [CrossRef]

27. Yan, X.; Jiang, Y. Numerical evaluation of thefog collection potential of electrostatically enhanced fog collector. *Atmos. Res.* **2021**, *248*, 105251. [CrossRef]

28. Zhang, H.; Huang, G.; Gong, C.; Yang, Y.; Pan, Y. Corona Discharge-Induced Water Droplet Growth in Air. *IEEE Trans. Plasma Sci.* **2020**, *48*, 2437–2441. [CrossRef]

29. Nouri, H.; Zouzou, N.; Moreau, E.; Dascalescu, L.; Zebboudj, Y. Effect of relative humidity on current–voltage characteristics of an electrostatic precipitator. *J. Electrost.* **2012**, *70*, 20–24. [CrossRef]

30. Wang, X.; You, C. Effect of humidity on negative corona discharge of electrostatic precipitators. *IEEE Trans. Dielectr. Electr. Insul.* **2013**, *20*, 1720–1726. [CrossRef]

31. Tan, Z. *Air Pollution and Greenhouse Gases: From Basic Concepts to Engineering Applications for Air Emission Control*; Springer: Singapore, 2014.

32. Leu, J.-S.; Jang, J.-Y.; Wu, Y.-H. Optimization of the wire electrode height and pitch for 3-D electrohydrodynamic enhanced water evaporation. *Int. J. Heat Mass Transf.* **2018**, *118*, 976–988. [CrossRef]

33. Ning, Z.; Cheng, L.; Shen, X.; Li, S.; Yan, K. Electrode configurations inside an electrostatic precipitator and their impact on collection efficiency and flow pattern. *Eur. Phys. J. D* **2016**, *70*, 126. [CrossRef]

34. Cao, R.; Tan, H.; Xiong, Y.; Mikulčić, H.; Vujanović, M.; Wang, X.; Duić, N. Improving the removal of particles and trace elements from coal-fired power plants by combining a wet phase transition agglomerator with wet electrostatic precipitator. *J. Clean. Prod.* **2017**, *161*, 1459–1465. [CrossRef]

35. Pan, X.; Zhang, Z.; Cui, L.; Zhang, Q.; Ma, C. Influence of heat exchange on the motion characteristics and mechanical behavior of fine particles in an electrostatic precipitator. *Powder Technol.* **2020**, *373*, 347–356. [CrossRef]